Combined Window-Filter Waveform Design With Transmitter-Side Channel State Information

Dong-Jun Han, *Student Member, IEEE*,
Jaekyun Moon, *Fellow, IEEE*,
Jy-yong Sohn, *Student Member, IEEE*,
Sunyoung Jo, *Student Member, IEEE*, and Jang Hun Kim

***Abstract*—In low-latency applications for 5G and beyond, precise synchronization becomes more challenging. In this correspondence, we generalized the analytical tool to design combined window-filter waveform, which can tolerate imperfect synchronization scenarios. Compared to the previous work focusing on an ideal channel, the generalized tool considers the effect of multipath fading with instantaneous or statistical channel state information at the transmitter (CSIT). The waveform designed by the proposed tool yields lower bit error rates compared to the design with no CSIT and other waveform candidates.**

***Index Terms*—5G, low-latency, universal filtered multi-carrier (UFMC), orthogonal frequency-division multiplexing (OFDM).**

I. Introduction

Latency is considered as one of the most important issues for next generation wireless communications (5G and beyond) [1]. Especially for vehicle-to-everything (V2X) communications in connected vehicle environments [2]–[4] or for Tactile Internet [5], achieving a round-trip latency of about 1 ms is desired. And to meet this requirement, one-way end-to-end latency in the physical layer should be as low as 100 μs [6]. Under such a tight latency constraint, precise synchronization becomes more challenging especially when the network supports massive number of low-cost devices with low-rate connections. The current orthogonal frequency-division multiplexing (OFDM) is sensitive to carrier frequency offset (CFO) and symbol timing offset (STO), which will be increasingly severe in such tight latency constraint scenarios.

Among various waveform proposals beyond OFDM, universal filtered multi-carrier (UFMC) has attracted considerable attention in both academia and industry [7]–[12]. Compared to OFDM, UFMC offers significantly lower out-of-band (OOB) emission by subband filtering. Compared to filter bank multi-carrier (FBMC) [13]–[16], UFMC uses relatively short time-domain filters making the scheme more suitable for low-latency communications [9]. UFMC also has a flexibility to support multiple services depending on the system requirements [10]. Such advantages make UFMC one of the promising waveform proposals beyond OFDM.

Manuscript received October 19, 2017; revised March 26, 2018 and May 21, 2018; accepted May 24, 2018. Date of publication June 4, 2018; date of current version September 17, 2018. This work was supported under Grant-in-aid of the Hanwha Systems. The review of this paper was coordinated by Dr. Ngoc-Dung Dao. *(Corresponding author: Dong-Jun Han.)*

D.-J. Han, J. Moon, J.-y. Sohn, and S. Jo are with the School of Electrical Engineering, Korea Advanced Institute of Science and Technology, Daejoen 34141, South Korea (e-mail: djhan93@kaist.ac.kr; jmoon@kaist.edu; jysohn1108@kaist.ac.kr; sun90015@kaist.ac.kr).

J. H. Kim is with the Hanwha Systems, Seongnam 13488, South Korea (e-mail: janghun.kim@hanwha.com).

Color versions of one or more of the figures in this paper are available online at http://ieeexplore.ieee.org.

Digital Object Identifier 10.1109/TVT.2018.2843346

Recently, a combined window-filter waveform was introduced in [18]. This waveform is based on UFMC, but it optimally combines Nyquist windowing with subband filtering under a fixed excess frame length constraint. The combined windowing/filtering allows simultaneous spectral shaping on both subcarrier and subband. It was shown that with less filter taps, the window-filter waveform gives better performances than optimized UFMC.

In previous work [18], filter and window length are optimized assuming an ideal channel, i.e., a delta function. Other previous works on UFMC filter design [11], [12] also considered an ideal channel. The main novelty of this paper is the design of combined window-filter waveform considering the effect of multipath fading. To the best of the authors' knowledge, this is the first work on filter optimization of UFMC-based waveform with channel state information (CSI) at the transmitter (CSIT) in asynchronous scenarios. Our contributions are summarized as follows: 1) By defining the l-specific error vectors of both filter and combined channel/filter, we derive in-band and out-of-band errors considering the effect of multipath channel. 2) Based on the error vectors, we obtain the interference power by specifying the Hermitian matrices in terms of channel coefficients (with instantaneous CSIT) or in terms of 2^{nd} order statistics for the channel (with statistical CSIT). Closed-form filter solutions are obtained with this matrices. 3) Finally, it is shown via simulations that the waveform designed with the generalized analytical tool improves BER performance in multipath fading scenarios. The notations used in this paper are summarized in the footnote.[1]

II. System Model

The system model of combined window-filter waveform in uplink multi-user scenario is shown in Fig. 1. A single-data-symbol transmission is considered which targets low-latency applications such as V2X communications or Tactile Internet, where the required latency should be achieved by short-burst transmissions. The multi-carrier system with overall N subcarriers are divided into B subbands, where each subband corresponds to a single user. Let $\mathbf{X}_i$ be the frequency-domain row vector of length N for the i-th subband, which has all zeros except for the subcarrier indices of the i-th subband. Each frequency-domain subcarrier symbols are assumed to be independent and have normalized power of 1. After N-point inverse discrete Fourier transform, $\mathbf{X}_i$ becomes $\mathbf{x}_i$ which is the time-domain row vector. Then, the last N_{cp} samples of $\mathbf{x}_i$ are attached in the front as a cyclic prefix (CP). After applying Nyquist window of $\mathbf{w} = [\mathbf{w}_1^{N_{cp}}\ \mathbf{1}_{N-N_{cp}}\ \mathbf{w}_{N_{cp}}^1]$, the signal becomes $\mathbf{y}_i$, which can be written as $\mathbf{y}_i = [(\mathbf{x}_i)_{N-N_{cp}}^{N-1} \circ \mathbf{w}_1^{N_{cp}}\ \ (\mathbf{x}_i)_0^{N-N_{cp}-1}\ \ (\mathbf{x}_i)_{N-N_{cp}}^{N-1} \circ \mathbf{w}_{N_{cp}}^1]$. The vectors $\mathbf{w}_1^{N_{cp}}$, $\mathbf{w}_{N_{cp}}^1$ represent window transition shapes com-

[1]**Notations:** $\mathbf{X}^*$, $\mathbf{X}^H$, tr$\{\mathbf{X}\}$ $\circ$, $*$, $\circledast$ denote conjugate, conjugate transpose, trace of matrix $\mathbf{X}$, entry-wise product, linear convolution, circular convolution, respectively. The symbol $\mathbf{x}_a^b$ represents a row-vector segment of elements $[x_a\ x_{a+1} \cdots x_b]$ for $a < b$, $[x_a\ x_{a-1} \cdots x_b]$ for $a > b$. The superscript " $\rightarrow k$" in $\mathbf{x}^{\rightarrow k}$ is to denote a right cyclic-shift of $\mathbf{x}$ by k positions (with a negative k meaning a left cyclic-shift). The symbols $\mathbf{1}_j$, $\mathbf{0}_j$ represent row vector segment of j consecutive 1 s and 0 s, respectively. $\mathbf{1}$ is a vector with full of 1 s. $\mathbf{0}_{m\times n}$, $\mathbf{I}_N$ denote m by n all-zero matrix, N by N identity matrix respectively. $\mathbb{1}_{\mathbf{A}}$ denotes 1 if event $\mathbf{A}$ is true, and 0 otherwise. An overbar denotes expectation.

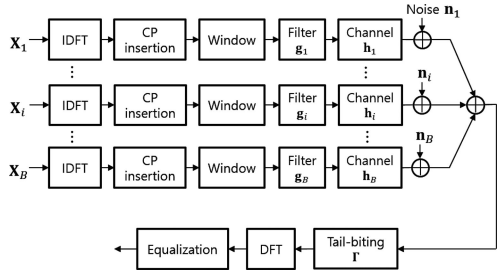

Fig. 1. Block diagram for transmitter and receiver of window-filter waveform in uplink multi-user scenario.

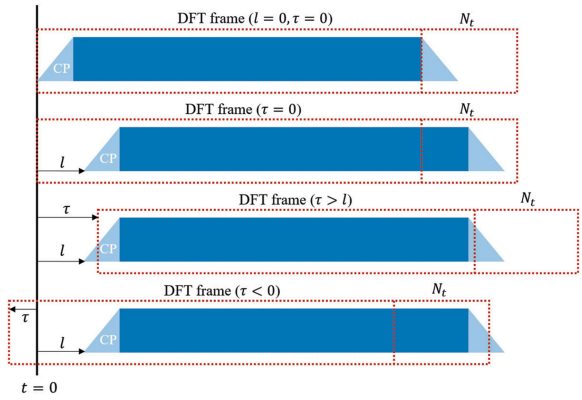

Fig. 2. Captured l-th multipath frames with different STOs.

pletely covering the CP and the last N_{cp} samples. Let $\mathbf{g}_i$, $\mathbf{h}_i$ be the subband filter with length L_g and channel impulse response with length L_h for subband i, respectively. Then, the signal of subband i after filtering and the channel becomes $\mathbf{z}_i = \mathbf{y}_i * \mathbf{v}_i$ where $\mathbf{v}_i = \mathbf{g}_i * \mathbf{h}_i$ is the combined filter/channel response with length $L_v = L_g + L_h - 1$. We set $N_t = N_{cp} + L_v - 1$, which is the minimum tail length needed to recover the transmitted symbols. We also define the excess length of the transmitted signal beyond the original symbol length of N, as $N_{ex} = N_{cp} + L_g - 1$. At the receiver, a tail-biting matrix

$$\mathbf{\Gamma} = \begin{bmatrix} & & & \mathbf{I}_N & & & \\ \mathbf{I}_{N_t} & & & \mathbf{0}_{N_t \times (N-N_t)} & & & \end{bmatrix}$$

is applied which takes the last N_t samples and add them to the first N_t samples. After summing up the transmit signals from all subbands, and applying tail-biting matrix and N-point discrete Fourier transform (DFT), the received signal finally becomes $\sum_{i=1}^{B}(\mathbf{z}_i + \mathbf{n}_i)\mathbf{\Gamma F}$ where $\mathbf{n}_i$ is the noise vector for the i-th subband and $\mathbf{F}$ is the DFT matrix with column k, $0 \le k \le N-1$, specified as $[1 \; e^{-j2\pi k/N} \; \cdots \; e^{-j2\pi(N-1)k/N}]^T$. It was shown in [18] that the noiseless received signal without CFO/STO, $\sum_{i=1}^{B} \mathbf{z}_i \mathbf{\Gamma F}$, can be perfectly recovered by using a symmetric window satisfying $\mathbf{w}_1^{N_{cp}} + \mathbf{w}_{N_{cp}}^1 = \mathbf{1}$.

III. Filter and Window Length Optimization

In this work, we would like to find the optimum filter $\mathbf{g}$ and window length N_{cp} to counter the effect of CFO/STO in multipath channel scenarios under a fixed excess frame length constraint N_{ex}. This paper considers raised-cosine window, but examining the effect of other kinds of window shapes remains as an interesting research topic. Since CSI may differ for each subband in uplink scenario, $\mathbf{g}$ and N_{cp} are optimized independently per subband. Therefore, we focus on a specific subband i, for analysis.

A. CFO/STO Induced Signal

For given normalized CFO of c and STO of τ, let $\mathbf{y}_{\tau,c}(l)$ be the l-th multipath signal (caused by combined filter/channel response) for the i-th subband. Index i is omitted in $\mathbf{y}_{\tau,c}(l)$ for notational simplicity. After tail-biting, we write $\mathbf{y}_{\tau,c}(l)\mathbf{\Gamma} = \mathbf{x}^{\rightarrow(l-\tau+N_{cp})} \circ \mathbf{d}(l) \circ \mathbf{q}$ where $\mathbf{q} = e^{j2\pi\tau c/N}[1 \;\; e^{j2\pi c/N} \;\; \cdots \;\; e^{j2\pi c(N-1)/N}]$, and $\mathbf{d}(l)$ represents a data capture frame due to CFO and STO. From the visual inspection of capture frames shown in Fig. 2, we can obtain

$$\mathbf{d}(l) = \begin{cases} [e^{j2\pi c} \times \mathbf{1}_{N_t} \; \mathbf{0}_{\rho-N_t} \; \mathbf{w}_1^{N_{cp}} \; \mathbf{1}_{N-N_{cp}-\rho}], \\ \qquad N_t + 1 \le \rho \le N - N_{cp} - 1 \\ [e^{j2\pi c} \times \mathbf{1}_{\rho} \; (\mathbf{w}_1^{N_t-\rho} + \mathbf{w}_{N_{cp}}^{N_{cp}-N_t+\rho+1} e^{j2\pi c}) \\ \qquad \mathbf{w}_{1+N_t-\rho}^{N_{cp}} \quad \mathbf{1}_{N-N_{cp}-\rho}], \\ \qquad N_t - N_{cp} + 1 \le \rho \le N_t \\ [e^{j2\pi c} \times \mathbf{1}_{\rho} \; \mathbf{w}_1^{N_{CP}} + \mathbf{w}_{N_{CP}}^1 e^{j2\pi c} \; \mathbf{1}_{N-N_{CP}-\rho}], \\ \qquad 0 \le \rho \le N_t - N_{cp} \\ [(\mathbf{w}_{|\rho|+1}^{N_{cp}} + \mathbf{w}_{N_{cp}-|\rho|}^1 e^{j2\pi c}) \; \mathbf{1}_{N-N_{cp}} \; \mathbf{w}_{N_{cp}}^{N_{cp}-|\rho|+1}], \\ \qquad -(N_{cp}-1) \le \rho \le -1 \\ [\mathbf{1}_{N-|\rho|} \; \mathbf{w}_{N_{cp}}^1 \; \mathbf{0}_{|\rho|-N_{cp}}], \; -N_t \le \rho \le -N_{cp} \end{cases} \quad (1)$$

where $\rho = l - \tau$. This equation is obtained in the previous work [18]. After N-point DFT, the signal becomes

$$\mathbf{y}_{\tau,c}(l)\mathbf{\Gamma F} = \mathbf{X} \circ \mathbf{P}(l - \tau + N_{cp}) \circledast \mathbf{A}(l) = \mathbf{X}\mathbf{P}_{l-\tau+N_{cp}}\mathbf{A}_l \quad (2)$$

where $\mathbf{P}(k) \triangleq [1 \; e^{-j2\pi k/N} \;\; \cdots \;\; e^{-j2\pi(N-1)k/N}]$ is a phase rotation vector, $\mathbf{A}(l) \triangleq [\mathbf{d}(l) \circ \mathbf{q}]\mathbf{F}$, $\mathbf{P}_j \triangleq \text{diag}(\mathbf{P}(j))$ and $\mathbf{A}_l$ is a circular convolution matrix having n-th cyclic shift of $\mathbf{A}(l)$ in the n-th row. Note that the l-th multipath signal with perfect synchronization, $\mathbf{y}(l)$, becomes $\mathbf{y}(l)\mathbf{\Gamma F} = \mathbf{X}\mathbf{P}_{l+N_{cp}}$ after tail-biting and DFT.

B. Error Calculations

By summing up the weighted signals at different delay positions, the distorted signal after tail-biting and DFT for a specific subband becomes $\sum_{l=0}^{L_v-1} v_l \mathbf{y}_{\tau,c}(l)\mathbf{\Gamma F}$, where v_l is the l-th tap of $\mathbf{v}_i$, the combined filter/channel response. Let $g_k e^{j2\pi\Omega_i k/N}$, $0 \le k \le L_g - 1$ be the k-th element of $\mathbf{g}_i$ where Ω_i is the center frequency of subband i and g_l is the l-th element of the corresponding filter $\mathbf{g}$ which is centered at the first frequency bin. Let h_k, $0 \le k \le L_h - 1$ be the k-th element of $\mathbf{h}_i$ which are independent for $\forall k$. We define a diagonal mask matrix $\mathbf{M}_{ob}$ that suppresses all signals inside the given subband plus the null subcarrier positions. By considering the multipath channel effects, the

out-of-band error is derived as

$$\begin{aligned}\mathbf{e}_{ob} &\triangleq \sum_{l=0}^{L_v-1} v_l \mathbf{y}_{\tau,c}(l)\mathbf{\Gamma F M}_{ob} = \sum_{l=0}^{L_v-1} v_l \mathbf{X P}_{l-\tau+N_{cp}} \mathbf{A}_l \mathbf{M}_{ob} \\ &= g_0[h_0\boldsymbol{\epsilon}_{ob}(0) + h_1\boldsymbol{\epsilon}_{ob}(1) + \cdots + h_{L_h-1}\boldsymbol{\epsilon}_{ob}(L_h-1)]\mathbf{M}_{ob} \\ &\quad + g_1 e^{j2\pi\Omega_i/N}[h_0\boldsymbol{\epsilon}_{ob}(1) + \cdots + h_{L_h-1}\boldsymbol{\epsilon}_{ob}(L_h)]\mathbf{M}_{ob} \\ &\quad \vdots \\ &\quad + g_{L_g-1} e^{j2\pi\Omega_i(L_g-1)/N}[h_0\boldsymbol{\epsilon}_{ob}(L_g-1) + h_1\boldsymbol{\epsilon}_{ob}(L_g) + \cdots \\ &\quad + h_{L_h-1}\boldsymbol{\epsilon}_{ob}(L_h+L_g-2)]\mathbf{M}_{ob} \\ &= \sum_{\tilde{l}=0}^{L_g-1} g_{\tilde{l}}[e^{j2\pi\Omega_i\tilde{l}/N} \sum_{r=0}^{L_h-1} h_r \boldsymbol{\epsilon}_{ob}(\tilde{l}+r)]\mathbf{M}_{ob} \quad (3) \\ &= \sum_{\tilde{l}=0}^{L_g-1} g_{\tilde{l}}\mathbf{f}_{ob}(\tilde{l})\mathbf{M}_{ob} \quad (4)\end{aligned}$$

where

$$\boldsymbol{\epsilon}_{ob}(l) \triangleq \mathbf{X P}_{l-\tau+N_{cp}} \mathbf{A}_l \quad (5)$$

$$\mathbf{f}_{ob}(\tilde{l}) \triangleq e^{j2\pi\Omega_i\tilde{l}/N} \sum_{r=0}^{L_h-1} h_r \boldsymbol{\epsilon}(\tilde{l}+r). \quad (6)$$

The vectors $\boldsymbol{\epsilon}_{ob}(l)$, $\mathbf{f}_{ob}(\tilde{l})$ can be viewed as l-specific out-of-band error vector of combined filter/channel, $\tilde{l}$-specific out-of-band error vector of filter, respectively.

For in-band, we assume that the phase rotation component τ can be compensated; then the captured signal is written as

$$\begin{aligned}\mathbf{y}_{\tau,c}(l)\mathbf{\Gamma F} &= \mathbf{X} \circ \mathbf{P}(l-\tau+N_{cp}) \circledast \mathbf{A}(l) \circ \mathbf{P}(\tau) \quad (7) \\ &= \mathbf{X P}_{l-\tau+N_{cp}} \mathbf{A}_l \mathbf{P}_\tau . \quad (8)\end{aligned}$$

Similar to the derivation of the out-of-band error considering the multipath channel effects, the in-band error becomes

$$\begin{aligned}\mathbf{e}_{ib} &\triangleq \sum_{l=0}^{L_v-1} v_l[\mathbf{A}(l)_0\mathbf{y}(l) - \mathbf{y}_{\tau,c}(l)]\mathbf{\Gamma F M}_{ib} \\ &= \sum_{l=0}^{L_v-1} v_l \mathbf{X P}_{l+N_{cp}}[\mathbf{A}(l)_0\mathbf{I} - \mathbf{P}_{-\tau}\mathbf{A}_l\mathbf{P}_\tau]\mathbf{M}_{ib} \quad (9) \\ &= \sum_{\tilde{l}=0}^{L_g-1} g_{\tilde{l}}[e^{j2\pi\Omega_i\tilde{l}/N} \sum_{r=0}^{L_h-1} h_r \boldsymbol{\epsilon}_{ib}(\tilde{l}+r)]\mathbf{M}_{ib} \quad (10) \\ &= \sum_{\tilde{l}=0}^{L_g-1} g_{\tilde{l}}\mathbf{f}_{ib}(\tilde{l})\mathbf{M}_{ib} \quad (11)\end{aligned}$$

where

$$\boldsymbol{\epsilon}_{ib}(l) \triangleq \mathbf{X P}_{l+N_{cp}}[\mathbf{A}(l)_0\mathbf{I} - \mathbf{P}_{-\tau}\mathbf{A}_l\mathbf{P}_\tau], \quad (12)$$

$$\mathbf{f}_{ib}(\tilde{l}) \triangleq e^{j2\pi\Omega_i\tilde{l}/N} \sum_{r=0}^{L_h-1} h_r \boldsymbol{\epsilon}_{ib}(\tilde{l}+r) \quad (13)$$

can be viewed as l-specific in-band error vector of combined window/filter and $\tilde{l}$-specific in-band error vector of filter. $\mathbf{A}(l)_0$ is the 0-th element of $\mathbf{A}(l)$ and $\mathbf{M}_{ib}$ is a diagonal matrix that suppresses all signals outside the given subband. By multiplying $\mathbf{A}(l)_0$ with each $\mathbf{y}(l)$, the error vector contains only the in-band distortion, not the signal difference.

Let $\mathbf{E}_{ob}, \mathbf{E}_{ib}$ be the matrices having vectors $\mathbf{f}_{ob}(\tilde{l}), \mathbf{f}_{ib}(\tilde{l})$ in its $\tilde{l}$-th row, respectively. Then, we can write $\mathbf{e}_{ob} = \mathbf{g}\mathbf{E}_{ob}\mathbf{M}_{ob}$, $\mathbf{e}_{ib} = \mathbf{g}\mathbf{E}_{ib}\mathbf{M}_{ib}$. Let $\mathbf{\Lambda}_{ob} = \overline{\mathbf{E}_{ob}\mathbf{M}_{ob}\mathbf{M}_{ob}^H\mathbf{E}_{ob}^H}$, $\mathbf{\Lambda}_{ib} = \overline{\mathbf{E}_{ib}\mathbf{M}_{ib}\mathbf{M}_{ib}^H\mathbf{E}_{ib}^H}$. Then, out-of-band and in-band interference power generated by a specific subband becomes

$$J_{ob} \triangleq \overline{||\mathbf{e}_{ob}||^2} = \mathbf{g}\overline{\mathbf{E}_{ob}\mathbf{M}_{ob}\mathbf{M}_{ob}^H\mathbf{E}_{ob}^H}\mathbf{g}^H = \mathbf{g}\mathbf{\Lambda}_{ob}\mathbf{g}^H \quad (14)$$

$$J_{ib} \triangleq \overline{||\mathbf{e}_{ib}||^2} = \mathbf{g}\overline{\mathbf{E}_{ib}\mathbf{M}_{ib}\mathbf{M}_{ib}^H\mathbf{E}_{ib}^H}\mathbf{g}^H = \mathbf{g}\mathbf{\Lambda}_{ib}\mathbf{g}^H . \quad (15)$$

To compute the signal power of the subband (which we would like to maximize), take only the signal part from (8). Then, considering the multipath channel, the distorted signal vector can be written as

$$\begin{aligned}&\sum_{\tilde{l}=0}^{L_g-1} g_{\tilde{l}}[e^{j2\pi\Omega_i\tilde{l}/N} \sum_{r=0}^{L_h-1} h_r \mathbf{A}(\tilde{l}+r)_0\mathbf{X P}_{\tilde{l}+r+N_{cp}}]\mathbf{M}_{ib} \quad (16) \\ &= \sum_{\tilde{l}=0}^{L_g-1} g_{\tilde{l}}\mathbf{s}(\tilde{l})\mathbf{M}_{ib}, \quad (17)\end{aligned}$$

where

$$\mathbf{s}(\tilde{l}) \triangleq \sum_{r=0}^{L_h-1} h_r \mathbf{A}(\tilde{l}+r)_0\mathbf{X P}_{\tilde{l}+r+N_{cp}} \quad (18)$$

is the $\tilde{l}$-specific signal vector of filter. Similar to the interference power, the signal power of subband i is defined as

$$Q \triangleq \mathbf{g}\overline{\mathbf{S}\mathbf{M}_{ib}\mathbf{M}_{ib}^H\mathbf{S}}\mathbf{g}^H = \mathbf{g}\mathbf{\Psi}\mathbf{g}^H, \quad (19)$$

where $\mathbf{S}$ is a matrix having vector $\mathbf{s}(\tilde{l})$ in its $\tilde{l}$-th row and $\mathbf{\Psi} \triangleq \overline{\mathbf{S}\mathbf{M}_{ib}\mathbf{M}_{ib}^H\mathbf{S}^H}$.

C. Optimization

Assuming imperfect synchronization of subband of interest, in-band and out-of-band interferences are considered with different CFO/STO as in [18]. Assuming in-band CFO/STO of c_{ib}, τ_{ib} and out-of-band CFO/STO of c_{ob}, τ_{ob}, the optimization problem for a specific i-th subband is formulated as

$$\max_{N_{cp}} \max_{\mathbf{g}} \frac{\mathbf{g}\mathbf{\Psi}(c_{ib},\tau_{ib})\mathbf{g}^H}{\mathbf{g}[\mathbf{\Lambda}_{ob}(c_{ob},\tau_{ob}) + \mathbf{\Lambda}_{ib}(c_{ib},\tau_{ib})]\mathbf{g}^H} \quad (20)$$

subject to $||\mathbf{g}||^2 = 1$. For given N_{cp}, the optimal filter is

$$\mathbf{g}_{opt} = c\,\boldsymbol{\phi}_{\max}\{[\mathbf{\Lambda}_{ob}(c_{ob},\tau_{ob}) + \mathbf{\Lambda}_{ib}(c_{ib},\tau_{ib})]^{-1}\mathbf{\Psi}(c_{ib},\tau_{ib})\} \quad (21)$$

directly by Rayleigh quotient result [19], where $\boldsymbol{\phi}_{\max}\{\mathbf{V}\}$ is defined as the eigenvector corresponding to maximal eigenvalue of $\mathbf{V}$ and c is a constant to satisfy $||\mathbf{g}_{opt}||^2 = 1$. The global optimum filter can be found by comparing the results for each N_{cp}. The elements of $\mathbf{\Lambda}_{ob}$, $\mathbf{\Lambda}_{ib}$, $\mathbf{\Psi}$ are specified by Proposition 1, where the proof is shown in Appendix.

Proposition 1: Let $\mathbf{B}_{ib}$, $\mathbf{B}_{ob}$, $\mathbf{B}_{nl}$ be the set of subcarrier indices for subband i, outside of subband i, null subcarriers beside subband i,

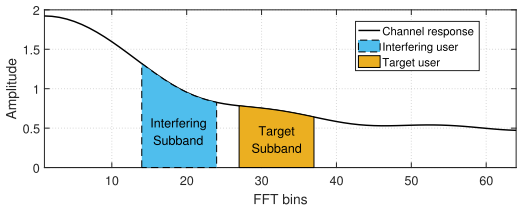

Fig. 3. Channel response and users in the frequency domain.

respectively. Let $b_i(k)=e^{j2\pi\Omega_i k/N}$ for $0 \le k \le N-1$. The (m,n)-elements of $\mathbf{\Lambda}_{ob}, \mathbf{\Lambda}_{ib}, \mathbf{\Psi}$ are

$$\Lambda_{ob}(m,n) = \sum_{p=0}^{L_h-1}\sum_{q=0}^{L_h-1}\sum_{l\in\mathbf{B}_{ib}}\sum_{k\in\mathbf{B}_{ob}\setminus\mathbf{B}_{nl}} h_p h_q^* b_i(m) b_i(n)^* \times e^{-j2\pi(m-n+p-q)l/N}\mathbf{A}^*(n+q)_{k-l}\mathbf{A}(m+p)_{k-l} \quad (22)$$

$$\Lambda_{ib}(m,n) = \sum_{p=0}^{L_h-1}\sum_{q=0}^{L_h-1}\sum_{l\in\mathbf{B}_{ib}}\sum_{\substack{k\in\mathbf{B}_{ib}\\k\neq l}} h_p h_q^* b_i(m) b_i(n)^* \times e^{-j2\pi(m-n+p-q)l/N}\mathbf{A}^*(n+q)_{k-l}\mathbf{A}(m+p)_{k-l} \quad (23)$$

$$\Psi(m,n) = \sum_{p=0}^{L_h-1}\sum_{q=0}^{L_h-1}\sum_{l\in\mathbf{B}_{ib}} h_p h_q^* b_i(m) b_i(n)^* \times e^{-j2\pi(m-n+p-q)l/N}\mathbf{A}^*(n+q)_0\mathbf{A}(m+p)_0 \quad (24)$$

for $m,n \in [0, L_g-1]$. $\mathbf{A}(m)_t$ denotes the t-th element of the vector $\mathbf{A}(m)$, and $\mathbf{A}(m)_{N+t} = \mathbf{A}(m)_t$ for the case $t<0$.

Proposition 1 was obtained with perfect CSIT. If only statistical CSI is given, each element of $\mathbf{\Lambda}_{ob}$, $\mathbf{\Lambda}_{ib}$, $\mathbf{\Psi}$ can be obtained directly by applying $\overline{h_p h_q^*} = \sigma_{h_p}^2 \mathbb{1}_{p=q}$ to Proposition 1. Here, $\sigma_{h_p}^2$ is the average power of the p-th channel tap.

In practical scenarios, each element of $\mathbf{\Lambda}_{ob}, \mathbf{\Lambda}_{ib}, \mathbf{\Psi}$ is averaged over distributions of CFO/STO since the exact CFO/STO values are unknown at the transmitter. Specific distributions such as Gaussian or uniform distribution can be considered.

IV. Numerical Results

In this section, numerical results are shown assuming an uplink two-user scenario. Two users occupy distinct subbands, where each subband is composed of eleven subcarriers. Two null subcarriers are used between subbands and statistical CSI are known at each transmitter. The user of interest is distorted by CFO/STO of c_{ib} and τ_{ib}, while the interfering user is distorted by CFO/STO of c_{ob} and τ_{ob}. Exponentially decaying power delay profile in [20] is used for multipath fading which fits well with indoor buildings and congested urban areas. Fig. 3 shows the channel response and the user model. DFT size of $N=128$ and uncoded quadrature phase shift keying (QPSK) is assumed for simulations. We compare our results with four other candidates: optimum window/filter with no CSIT (optimized assuming an ideal channel), OFDM using raised cosine window, UFMC using the Dolph-Chebyshev filter with side-lobe attenuation of 50 dB and OFDM with a CP. CP length of OFDM is set to N_{ex} for fair comparisons.

Assuming multipath channel length of $L_h=6$ and $c_{ib}=0.1, \tau_{ib}=-4, c_{ob}=0.2, \tau_{ob}=-8$, Fig. 4 shows the BER performance for the target user. Window lengths and filters are optimized for this fixed scenario. Two excess frame length constraints are considered: 1) $N_{ex}=12$, which is less than 10% of the DFT size for low-latency communications, and 2) $N_{ex}=16$, which is a less tighter constraint. As in the results of [18], [21], there are some error floors in the BER curves due effects of CFO/STO. The optimum design with CSIT gives improved performance compared to the design with no CSIT and others. Fig. 5 shows the block error rate (BLER) performance using Bose-Chaudhuri-Hocquenghem (BCH) code, which shows a great performance for short block lengths [22]. Assuming 2-error-correcting $(15,7)$ BCH code and $N_{ex}=12$, it can be seen that the design with CSIT achieves BLER of 10^{-6} at E_b/N_0 25 dB while the others do not.

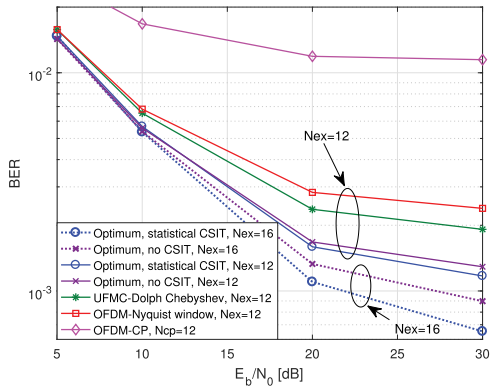

Fig. 4. BER for $c_{ib}=0.1$, $\tau_{ib}=-4$, $c_{ob}=0.2$, $\tau_{ob}=-8$. Filters are designed for this fixed scenario.

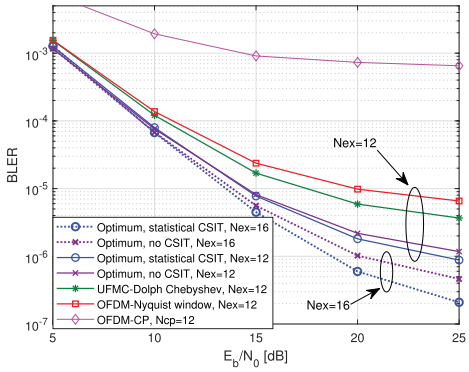

Fig. 5. BLER for $c_{ib}=0.1$, $\tau_{ib}=-4$, $c_{ob}=0.2$, $\tau_{ob}=-8$. BCH code is used and filters are designed for this fixed scenario.

Performance is also studied with the filters optimized over distributions of CFO/STO. Consider uniform distributions of CFO/STO over a range of $c_{ib} \in [-0.1, 0.1], \tau_{ib} \in [-6, 6], c_{ob} \in [-0.2, 0.2], \tau_{ob} \in [-13, 13]$. Assuming multipath channel length of $L_h=6$, the optimum filter length becomes $L_g=3$ for both $N_{ex}=12$, 16, which leads to a system with lower transmitter complexity compared to UFMC. Using the filters optimized for this uniform CFO/STO scenario, Fig. 6 shows the uncoded BER of the target user assuming $c_{ib}=0.1$, $\tau_{ib}=6$, $c_{ob}=0.2$, $\tau_{ob}=10$. Since OFDM with CP does not have performance losses for positive STOs (less than N_{cp}), it gives similar performance compared to UFMC with $N_{ex}=12$. Again, the optimum design with CSIT gives the best BER performance. The results indicate the advantage of the design with CSIT, which has improved robustness against CFO/STO compared to the design with no CSIT and reduced transmitter complexity compared to UFMC.

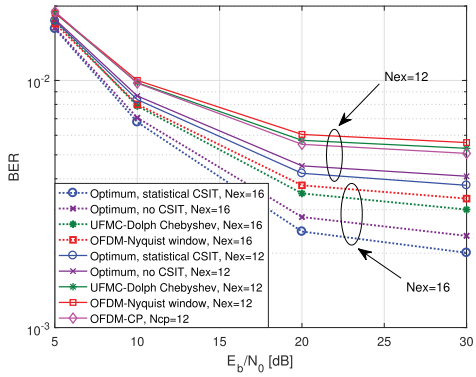

Fig. 6. BER for $c_{ib} = 0.1, \tau_{ib} = 6, c_{ob} = 0.2, \tau_{ob} = 10$. Filters are designed for uniform distributions of in-band and out-of-band CFO/STO.

V. Conclusion

A generalized analytical tool was established to design a combined window-filter waveform in multipath fading environments. The proposed design improves BER performance compared to the design with no CSIT and other schemes. This tool can be used for any excess frame length constraints, and for any multipath channel scenarios with CSIT.

Appendix

Proof of Proposition 1: From $\mathbf{\Lambda}_{ob} = \overline{\mathbf{E}_{ob}\mathbf{M}_{ob}\mathbf{M}_{ob}^H\mathbf{E}_{ob}^H}$,

$$\begin{aligned}
&\Lambda_{ob}(m,n) \\
&= \overline{\boldsymbol{f}_{ob}(m)\mathbf{M}_{ob}\mathbf{M}_{ob}^H\boldsymbol{f}_{ob}(n)^H} \\
&= \left[\mathrm{tr}\left\{\mathbf{M}_{ob}^H\overline{\boldsymbol{f}_{ob}^H(m)\boldsymbol{f}_{ob}(n)}\mathbf{M}_{ob}\right\}\right]^* \\
&= e^{j2\pi\Omega_i(m-n)/N}\left[\mathrm{tr}\left\{\mathbf{M}_{ob}^H\sum_{p=0}^{L_h-1}\sum_{q=0}^{L_h-1}h_p^*h_q\right.\right. \\
&\qquad\left.\left.\times\overline{\boldsymbol{\epsilon}_{ob}^H(m+p)\boldsymbol{\epsilon}_{ob}(n+q)}\mathbf{M}_{ob}\right\}\right]^* \\
&= b_i(m)b_i(n)^*\left[\mathrm{tr}\left\{\mathbf{M}_{ob}\sum_{p=0}^{L_h-1}\sum_{q=0}^{L_h-1}h_p^*h_q\mathbf{A}_{m+p}^H\mathbf{P}_{m+p-\tau+N_{cp}}^H\right.\right. \\
&\qquad\left.\left.\times\mathbf{M}\mathbf{P}_{n+q-\tau+N_{cp}}\mathbf{A}_{n+q}\right\}\right]^* \\
&= b_i(m)b_i(n)^*\left[\mathrm{tr}\left\{\sum_{p=0}^{L_h-1}\sum_{q=0}^{L_h-1}h_p^*h_q\mathbf{A}_{n+q}\mathbf{M}_{ob}\mathbf{A}_{m+p}^H\right.\right. \\
&\qquad\left.\left.\times\mathbf{P}_{m-n+p-q}^H\mathbf{M}\right\}\right]^*
\end{aligned}$$

where $\mathbf{M} = \overline{\mathbf{X}^H\mathbf{X}}$ is a diagonal matrix with 1s in (n,n)-element for $\forall n \in \mathbf{B}_{ib}$ and 0 s elsewhere. The (l,k)-th element of $\mathbf{A}_{n+q}\mathbf{M}_{ob}$ is given by $\mathbf{A}(n+q)_{k-l}$ for $k \in \mathbf{B}_{ob}\backslash\mathbf{B}_{nl}$ while being zero otherwise. The (k,l)-th element of $\mathbf{A}_{m+p}^H$ is given by $\mathbf{A}^*(m+p)_{k-l}$. So the (l,l)-th element of $\mathbf{A}_{n+q}\mathbf{M}_{ob}\mathbf{A}_{m+p}^H\mathbf{P}_{m-n+p-q}^H$ can be written as $\sum_{k\in\mathbf{B}_{ob}\backslash\mathbf{B}_{nl}} e^{j2\pi(m-n+p-q)l/N}\mathbf{A}(n+q)_{k-l}\mathbf{A}^*(m+p)_{k-l}$. By taking sum over l,p,q and taking the conjugate, we subsequently get (22). The proof for $\Lambda_{ib}(m,n)$, $\Psi(m,n)$ are similar to the one for $\Lambda_{ob}(m,n)$.

References

[1] J. G. Andrews *et al.*, "What will 5G be?," *IEEE J. Sel. Areas Commun.*, vol. 32, no. 6, pp. 1065–1082, Jun. 2014.

[2] S. Lee, S. Hyeon, J. Kim, H. Roh, and W. Lee, "The useful impact of carrier aggregations: A measurement study in South Korea for commercial LTE-advanced networks," *IEEE Veh. Technol. Mag.*, vol. 12, no. 1, pp. 55–62, Mar. 2017.

[3] G. Araniti, C. Campolo, M. Condoluci, A. Iera, and A. Molinaro, "LTE for vehicular networking: A survey," *IEEE Commun. Mag.*, vol. 51, no. 5, pp. 148–157, May 2013.

[4] J. Kim, S.-C. Kwon, and G. Choi, "Performance of video streaming in infrastructure-to-vehicle telematic platforms with 60-GHz radiations and IEEE 802.11 ad baseband," *IEEE Trans. Veh. Technol.*, vol. 65, no. 12, pp. 10111–10115, Dec. 2016.

[5] M. Simsek, A. Aijaz, M. Dohler, J. Sachs, and G. Fettweis, "5G-Enabled Tactile Internet," *IEEE J. Sel. Areas Commun.*, vol. 34, no. 3, pp. 460–473, Mar. 2016.

[6] G. Wunder *et al.*, "5GNOW: Non-orthogonal, asynchronous waveforms for future mobile applications," *IEEE Commun. Mag.*, vol. 52, no. 2, pp. 97–105, Feb. 2014.

[7] V. Vakilian, T. Wild, F. Schaich, S. ten Brink, and J.-F. Frigon, "Universal-filtered multi-carrier technique for wireless systems beyond LTE," in *Proc. IEEE Globecom Workshop*, 2013, pp. 223–228.

[8] Y. Chen, F. Schaich, and T. Wild, "Multiple access and waveforms for 5G: IDMA and universal filtered multi-carrer," in *Proc. IEEE 79th Veh. Technol. Conf.*, 2014, pp. 1–5.

[9] F. Schaich, T. Wild, and Y. Chen, "Waveform contenders for 5G suitability for short packet and low-latency transmissions," in *Proc. IEEE 79th Veh. Technol. Conf.*, 2014, pp. 1–5.

[10] L. Zhang, A. Ijaz, P. Xiao, A. Quddus, and R. Tafazolli, "Subband filtered multi-carrier systems for multi-service wireless communications," *IEEE Trans. Wireless Commun.*, vol. 16, no. 3, pp. 1893–1907, Mar. 2017.

[11] X. Wang, T. Wild, F. Schaich, and A. F. Dos Santos, "Universal filtered multi-carrier with leakage-based filter optimization," in *Proc. 20th Eur. Wireless Conf.*, 2014, pp. 1–5.

[12] X. Wang, T. Wild, and F. Schaich, "Filter optimization for carrier frequency and timing offsets in universal filtered multi-carrier system," in *Proc. IEEE 79th Veh. Technol. Conf.*, 2015, pp. 1–6.

[13] B. Farhang-Boroujeny, "OFDM versus filter bank multicarrier," *IEEE Signal Process. Mag.*, vol. 28, no. 3, pp. 92–112, May 2011.

[14] M. Bellanger *et al.*, "FBMC physical layer: A primer," in PHYDYAS FP7 Project Document, Jan. 2010.

[15] L. Zhang, P. Xiao, A. Zafar, A. Quddus, and R. Tafazolli, "FBMC system: An insight into doubly dispersive channel impact," *IEEE Trans. Veh. Technol.*, vol. 66, no. 5, pp. 3942–3956, May 2017.

[16] H. Lee, B. Kwon, D. Jeon, S. Kim, and S. Lee, "Mutual interference analysis of FBMC-based return channel for bidirectional T-DMB system," *IEEE Trans. Veh. Technol.*, vol. 66, no. 5, pp. 3829–3842, May 2017.

[17] A. Aminjavaheri, A. Farhang, A. RezazadehReyhani, and B. Farhang-Boroujeny, "Impact of timing and frequency offsets on multicarrier waveform candidates for 5G," in *Proc. IEEE Signal Process. Edu. Workshop*, Aug. 2015, pp. 178–183.

[18] D.-J. Han, J. Moon, D. Kim, S.-Y. Chung, and Y. H. Lee, "Combined subband-subcarrier spectral shaping in multi-carrier modulation under the excess frame length constraint," *IEEE J. Sel. Areas Commun.*, vol. 35, no. 6, pp. 1339–1352, Jun. 2017.

[19] G. Golub and C. V. Loan, *Matrix Computations*. vol. 3. Baltimore, MD, USA: The Johns Hopkins Univ. Press, 2012.

[20] M. K. Simon and M. Alouini, *Digital Communication Over Fading Channels*, 2nd ed. New York, NY, USA: Wiley, 2005.

[21] S. Wang, J. S. Thompson, and P. M. Grant, "Closed-form expressions for ICI/ISI in filtered OFDM systems for asynchronous 5G uplink," *IEEE Trans. Commun.*, vol. 65, no. 11, pp. 4886–4898, Nov. 2017.

[22] M. Shirvanimoghaddam *et al.*, "Short block-length codes for ultra-reliable low-latency communications," 2018. [Online]. Available: https://arxiv.org/abs/1802.09166